Electrochimica Acta 219 (2016) 363–376

Contents lists available at ScienceDirect

Electrochimica Acta

journal homepage: www.elsevier.com/locate/electacta

Electroactive polymers made by loading redox ions inside crosslinked polymeric hydrogels. Effects of hydrophobic interactions and solvent dynamics

María Victoria Martinez, Mariano M. Bruno, María Cristina Miras, Cesar A. Barbero*

Department of Chemistry, Universidad Nacional de Río Cuarto-CONICET, Ruta 8 y 36 Km 601, X5804ZAB, Río Cuarto, Córdoba, Argentina

ARTICLE INFO

Article history:
Received 10 July 2016
Received in revised form 29 September 2016
Accepted 1 October 2016
Available online 4 October 2016

Keywords:
Electroactive polymers
Hydrogels
Semi-infinite diffusion
Heterogeneous charge transfer
Redox complexes
Hydrophobic interactions

ABSTRACT

Electroactive polymers are made by loading redox complexes inside different polymeric crosslinked hydrogels. A redox cation (tris(phenanthroline)iron(II) (TPFeII) is sorbed in anionic, neutral and cationic hydrogels while redox anions (ferricyanide) is taken up inside an anionic hydrogel. Moreover, a redox anion (nitrite) and a cation (TPFeII) are simultaneously absorbed in an anionic hydrogel. Homopolymeric hydrogels of 2-acrylamidopropanesulfonic acid (PAMPS), acrylic acid (PAA) or (3-acrylamidopropyl) trimethylammonium chloride) (PAPMTAC), crosslinked with bisacrylamide, are synthesized by radical polymerization. The same method is used to produce a 1:1 copolymeric hydrogel of acrylic acid and 2-acrylamidopropanesulfonic acid (PAA-co-AMPS). The physicochemical properties of the hydrogels are evaluated by measuring the swelling kinetics, in the same conditions of the electrochemical measurements. The cyclic voltammetric response of all electroactive polymers show quasireversible electron transfer (E_{qrev} mechanism) while the hydrogel loaded with TPFeII and nitrite show a catalyzed oxidation ($E_{qrev}C$ mechanism). The electrochemical parameters (diffusion coefficient and charge transfer constant) of TPFeII loaded inside PAMPS, PAA and PAA-co-AMPS are measured using chronoamperometry and digital simulation of the cyclic voltammetry. The Stokes-Einstein equation is used to calculate the effective viscosity of the hydrogel matrixes using the diffusion coefficients of a redox complex (TPFeII) determined inside the hydrogels and the same parameters determined in aqueous solution. The calculated viscosity correlates, with a negative slope, with the swelling rate constant of the hydrogel matrix. The heterogeneous charge transfer of the redox complex inside ionomers (PAMPS and PAA-co-PAMPS) is nearly as fast as in solution, while the charge transfer inside the neutral PAA is ca. 100 times smaller. The measured charge transfer constants correlate with the calculated viscosity, revealing the effect of solvent dynamics on the charge transfer, according to Marcus theory for strongly adiabatic electron transfer. In that way, it is shown that the electrochemical measurements are able to monitor the local solvation properties of the hydrogel matrix. These results suggest novel ways to produce electroactive polymers by loading redox active substances inside hydrogels, even when the hydrogel matrix is neutral or bear the same charge than the redox probe. The redox complexes are present as dilute solutions and the hydrogel dimensions fulfill the semi-infinite diffusion boundary conditions. Therefore, the data analysis can be performed using the theoretical framework for electrochemical measurements in liquid solvents.

© 2016 Elsevier Ltd. All rights reserved.

1. Introduction

Electroactive polymers are materials of great interest both for basic understanding [1], and technological applications [2]. Lyons, [3] define three main kinds of electroactive polymers, which are: conducting polymers, redox polymers and loaded ionomers. All contain entities that can exchange electrons with a conductive substrate giving rise to an electrochemical response. In redox polymers the electrons are transported by electron hoping between neighboring redox centers [4]. In loaded ionomers the electrons are transported across the materials by physical diffusion/migration of the loaded redox species [5,6], while a contribution of electron hoping between neighboring redox centers to charge transport is possible if the internal concentration

* Corresponding author.
E-mail address: cbarbero@exa.unrc.edu.ar (C.A. Barbero).

http://dx.doi.org/10.1016/j.electacta.2016.10.007
0013-4686/© 2016 Elsevier Ltd. All rights reserved.

is high enough [7]. Conducting polymers could act as three dimensional electrodes since they have intrinsic electronic conductivity [8]. However, if the conductive matrix is not electrically connected, electron hopping between conducting domains could occur.

In all electroactive polymers mass transport of mobile counterions/coions inside the polymer need to be coupled with electron transport to maintain electroneutrality. Therefore, some concentration of mobile ions is required to be present inside the polymer. While there are neutral redox polymers (e.g. polivinylferrocene), the material insert ions during oxidation and a process of loading with electrolyte solution ("break in") is observed [9]. In the case of conducting polymers, they are usually produced in the salt state, where an stoichiometric amount of counterions is present. However, when the polymers are electrochemically reduced, the amount of counterions decreases and the film become neutral. This is likely to be the one of the reasons that the oxidation depends on the level of reduction, the so called "memory effect" [10,11]. In the case of loaded ionomers, the ionic conductivity is high due to the presence of large concentrations of mobile counterions of the fixed charges in the ionomer. Since in this paper we propose to study not only loaded ionomers but loaded neutral hydrogels, the situation can be different and should be taken into account [12].

The electrochemistry response of electroactive polymers depart from a simple model of a single electron transfer at the electrode/polymer interface coupled to some form of charge transport across the polymer sample [1,2]. In the case of redox moieties covalently linked to the polymer, the mobility and microenvironment can affect the concentration/potential relationship [13]. While it is usually assumed that the linked redox species (e.g. ferrocene) has the same physicochemical properties than the same species in solution, this is usually not the case [14].

Moreover, since usually the concentration of redox sites is usually large (>0.1 M), even in the case of loaded ionomers with well-known redox species, infinite dilution conditions cannot be assumed and therefore activity effects could be present. The usual way to measure electrochemistry of electroactive polymers is depositing a film of the material, containing redox moieties, on a solid electrode (e.g. glassy carbon) [15].

In the case of loaded ionomers, the redox species is then sorbed from aqueous solution inside the deposited film [16].

The polymer film has to be wetted by the solvent but the whole polymer film needs to be insoluble in the solution. This is achieved by using polyelectrolytes with hydrophobic domains which crosslink the film during deposition by solvent evaporation (e.g. Nafion®) or by chemical reaction of the polymer chains (e.g. polyvinylpyridine) with a crosslinker (e.g. 1,4-dichlorobutane). Another method involves layer-by-layer self-assembly of opposite charge polyelectrolytes [17]. In the case of conducting polymers, the monomer is oxidized on the electrode forming a slightly soluble polymer which adsorbs on the electrode, while following layer are retained by non-covalent interaction between polymer chains [18]. Those methods are difficult to control and the deposition conditions strongly influence the solid state properties [19].

Moreover, the characterization of solid state properties of the polymers like swelling, porosity, elasticity, is quite difficult due to the small dimensions of the polymer films [20]. Therefore, it is usually assumed that the properties are the same that bulk materials which is usually not the case due to different formation procedures. Additionally, deposited films could show large difference between the layers closer to the substrate (electrode) and those in the bulk of the film [21]. The use of polymer films deposited on electrodes makes the electrochemistry easy because the hydrogel is contacted in the innermost layer with the electrode and the outside layer is exposed to the solution [22]. However, in thin films the semi-infinite boundary condition, usually assumed in liquid solutions, is not necessarily fulfilled. The thickness of the diffusion layer inside the film depends on the mass transport parameters, the time frame of the measurement (e.g. scan rate in cyclic voltammetry) and the thickness of the film. Three regimes can exist: i) a semi-infinite layer with diffusion; ii) a thin layer with complete electrolysis and (iii) a finite diffusion layer. While the (i) and (ii) are amenable for data analysis, (iii) has a complex dependence on the thickness and morphology [23]. Indeed, Leddy and coworkers have recently proposed a diagnostic criteria for cyclic voltammetry which allows to know in which regime is the experimental measurement [24]. In any case, the determination of diffusion coefficient requires measuring at short times (high scan rates in cyclic voltammetry) where other effects (capacitive and heterogeneous charge transfer) are usually important [25]. Since thin layer conditions can be achieved, at long times (chronocoulometry) or small scan rates (cyclic voltammetry) the number of moles of active species can be calculated from the measured charge. However, to calculate the concentration, the thickness needs to be known. This value is usually done ex-situ and likely does not represent the in-situ thickness [5].

In the present work we describe a new system, related to loaded ionomers with redox species, where well known redox species are absorbed, at low concentrations, inside neutral or charged bulk hydrogels. The hydrogel samples are thick enough to assure semi-infinite conditions.

Hydrogels made of crosslinked polymer matrixes are interesting materials for different technological applications: drug release, chemical actuators, sensors, etc. [26,27]. Polyacrylamides, [28] and related materials (e.g. poly(acrylic) acid) have been extensively studied [29]. The materials can be easily synthesized by radical polymerization in water or similar solvents [30]. An additional advantage is the widespread availability of monomers combined with the feasibility of copolymerization allowing to create crosslinked polymers bearing different functional groups. In that way, different chemical structures can be easily built [31]. Moreover, hydrogels responsive to chemical or electrochemical oxidation have been devised [32]. However, the electrochemical properties of such materials have been scarcely studied.

In ionomers (e.g. Nafion®) loaded with redox species (e.g. $Fe(bpy)_3^{2+}$) the redox couple could physically diffuse as in a dilute solution. However, when the concentration of redox species is large enough, neighboring species of different redox state could exchange electrons; such a process could contribute to mass transport or even dominate it. The formalism to model the phenomena was developed by Dahms [33], and Ruff [34], for concentrated solutions of redox species in liquids. In the case of polymers, besides the bulk concentration, the possibility of phase separation due between hydrophobic and hydrophilic domains in the hydrogel has to be considered. Indeed, in Nafion® the proton diffusion trough the membrane does not occur as a bulk diffusion process but as a percolation controlled process between hydrophilic domains containing $-SO_3^-H^+$ groups, which are surrounded by hydrophobic domains containing fluorinated chains [35]. Such considerations have been taken into account by Leddy and coworkers for the understanding of the electrochemistry of redox couples (e.g. $Ru(bpy)_3^{2+}$) in electrodes modified with Nafion® films [36].

Unlike films deposited on electrodes, macroscopic hydrogels can be easily characterized in terms of chemical structure [37], swelling capacity [38], porosity [39], mechanical properties [40], and inner concentration [41]. Previously, we found that metallic complexes (e.g. $Ru(bpy)_3^{2+}$) are strongly retained inside the polymeric hydrogels, even neutral ones [41]. Therefore, electroactive hydrogels could be produced not only by loading redox ions on ionomers bearing groups with the opposite charge but also

neutral or even ionomers with the same charge. The presence of fixed charges inside the hydrogel increase the ionic conductivity due to the presence of mobile counterions, relevant experimental parameter in electrochemistry [42]. Moreover, since they are synthesized as macroscopic samples the hydrogels are homogenous and the concentration of redox species can be measured independently by well-known analytical methods.

Recently [43], we have shown that it is possible to study the electrochemical behavior of tris(phenanthroline)iron(II) loaded inside a charged hydrogel matrix (poly(acrylamide-co-(2-acrylamidopropansulfonic acid)). The simple experimental set-up uses, as working electrode, a flat glassy carbon electrode pressed onto the hydrogel surface, while the reference and counterelectrode are both set in the electrolyte solution where the hydrogel is immersed. It was shown that the complex loaded inside the hydrogel show a single electron step when an excess phenanthroline is used. However, when a stoichiometric amount of ligand is used the complex is in equilibrium with free iron which is catalytically oxidized by the tris(phenanthroline)iron(III) species. The diffusion coefficient of the redox complex was determined by chronoamperometry. The simplicity of the approach prompts us to use the method to study in depth different hydrogels, both charged and neutral.

In the present work, we produce different hydrogels containing anionic groups (-SO_3^-) such as poly(2-acrylamidopropansulfonic acid) (PAMPS) and neutral groups such as acrylic acid(in acid pH). A copolymer which contain both kinds of groups is also synthesized (poly(acrylic-co-(2-acrylamidopropansulfonic) acid), PAA-co-AMPS). The hydrogels are characterized in terms of structure, swelling capacity and swelling rate. Then, electroactive polymers are made by loading a positively charged redox complex: (tris (phenanthroline)iron(II), TPFeII), both on the ionomers bearing negative charges (PAMPS y PAA-co-AMPS), and neutral hydrogels (PAA at pH = 3). The mass transport of the redox complex inside the hydrogels is measured using chronoamperometry. The rate of mass transport depends on the physicochemical properties of the hydrogel matrixes. The electrochemistry of redox complexes inside the hydrogels show "fast" or "slow" quasireversible charge transfer, depending on the hydrogel structure. It seems that local viscosity effects affect the charge transfer.

Another electroactive polymer is made by loading an anionic complex (ferricyanide, $Fe(CN)_6^{-3}$) inside an anionic hydrogel (PAMPS). Analogously, nitrite ions are absorbed inside an electroactive polymer made by loading TPFeII in PAMPS The nitrite is catalytically oxidized inside the bulk of the hydrogel where is sorbed. The successful loading of ferricyanide and nitrite is surprising since Donnan exclusion of anions is expected by the fixed $-SO_3^-$ groups in PAMPS. It seems that hydrophobic interactions are able to overcome the electrostatic repulsion. Based on this results, the loading and electrochemical activity of TPFeII (bearing positive charges) inside a cationic polyelectrolyte (poly ((3-acrylamidopropyl)trimethylammonium chloride), PAPMTAC) is successfully tested.

In that way, the electrochemical behavior of different electroactive polymers made by loading redox complexes inside charged or neutral hydrogels is studied. Since the polymer samples are thick (>3 mm), the semi-infinite boundary condition is fulfilled. Moreover, since the concentrations could be kept low, infinite dilution conditions are also fulfilled. The approach seems to give a new way to produce electroactive polymers.

2. Experimental

2.1. Materials

All chemicals are of analytical quality. Millipore (18.2 MΩ cm) purified water was used to prepare the solutions.

2.2. Synthesis of hydrogel matrix

The different hydrogels were synthesized via free-radical copolymerization of monomers: 2-acrylamido-2-methylpropanesulfonic acid (AMPS) (Scientific Polymer Products), acrylic acid (Sigma-Aldrich) and (3-acrylamidopropyl)trimethylammonium chloride (Sigma-Aldrich). The structures of the polymer chains constituting the hydrogels are shown in Scheme 1.

The total monomer concentration is 2 M. N,N′-methylenebisacrylamide (BIS) (Aldrich) was used as cross-linker agent. The radical polymerization was initiated thermally by 2,2'-Azobis(2-methylpropionamidine) dihydrochloride (V50) (Aldrich). This is decomposed at temperature higher than 56 °C to generate free radicals. In this synthesis was used a buffer solution pH = 10 as solvent. The monomers and cross-linker (BIS, 2% moles based on copolymer) were placed in a tube and added the buffer until a final volume of 4 ml, then the solution was purged by bubbling with N_2 gas and the initiator (V50 (0.003 g ml^{-1})) is added. The polymerization was carried out in a sealed glass tube in a water bath at 60 °C to allow the initiator decomposition. The tubes were left in the bath until gelation (ca. 15 minutes). When the polymerization was completed, the hydrogels were immersed in distilled water at room temperature for 48 h and the water was renewed several times in order to remove unreacted chemicals.

2.3. Structural characterization

The FTIR spectra of the different hydrogels (Fig. S1, supplementary information) show bands related with the functional groups

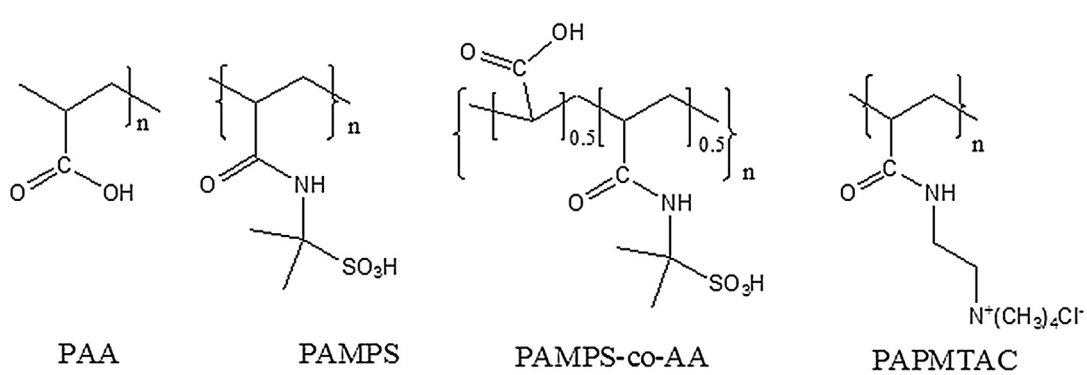

Scheme 1. Chemical structure of the polymer hydrogels.

present in the different monomer units, indicating that both the two homopolymers and the copolymers have the structure

2.4. Swelling measurements

Dry hydrogel samples previously washed and weighed were placed in water at room temperature. After 24 h (necessary time to achieve the swelling equilibrium condition) the samples were removed from solution, superficially dried with tissue paper and weighed in an analytic balance. The measurements were repeated until sample achieved the constant weight. The swelling percentage (% *Sw*) is calculated as:

$$\%Sw = \frac{(W_{eq} - W_{dry})}{W_{dry}} x100 \quad (1)$$

where W_{eq} represents the weight of swollen hydrogel in equilibrium and W_{dry} is the weight of dry hydrogel. Every data of % *Sw* obtained was the averaged of five measurement with absolute error around ±150. This characterization was made to the complete library of hydrogels.

2.5. Complex loading in the hydrogels

The swollen hydrogels are contacted with redox complex (e.g. tris(phenanthroline)iron(II)) solutions of a given concentration for 24–48 hours. Traces of hydrazine are added to avoid the Fe^{2+} to Fe^{3+} oxidation, and a slight excess of phenanthroline is added to avoid complex hydrolysis [43]. The loading of ferricyanide ($Fe(CN)_6^{-3)}$ or nitrite ions is carried out in 10 mM solutions of each anion during 48 hs.

2.6. Partition coefficient

The partition coefficient (P_{molal}) is defined the relation of molal concentration (number of moles of TPFeII in a kg of media (solvent or hydrogel)) between the solution and the dry hydrogel. The number of moles inside the hydrogel is measured, using UV–vis spectrophotometry, from the decrease in concentration of the solution when the gel is equilibrated with the external solution. The large changes in volume upon swelling preclude the use of molar concentrations.

$$P_{molal} = \frac{[Fe(phenanthroline)_3^{2+}]_{hydrogel}}{[Fe(phenanthroline)_3^{2+}]_{solution}} \quad (2)$$

From the partition coefficient and using the actual volume of the hydrogel, measured using Arquimedes's principle, the inner concentration is calculated in each case.

2.7. Electrochemical measurements

A 3 mm glassy carbon disc, inserted in a Kel-F shroud and contacted in the back with silver paste, was used as working electrode. The reference was a silver wire (0.5 mm) where a thick layer of AgCl was deposited by anodic oxidation in 1 M KCl solution. The coiled wire is placed inside a glass Luggin capillary filled with saturated KCl solution. To assure a uniform potential field, the counterelectrode is set as a Pt grid beneath the hydrogel piece. (see Scheme 1). A photograph of the experimental set-up is shown in the supplementary information (Fig. S2). The electrochemical experiments were controlled by a computer controlled potentiostat (Autolab PGSTAT30, Ecochemie). Cyclic voltammetry experiments were carried between 0.5 V and 1.2 V at different scan rates. Either with the electrode exposed to the solution or with the electrode gently pressed onto the hydrogel. No effect of pressure was observed, once a clear mechanical contact between the electrode and the hydrogel is observed. In analog fashion, chronoamperometric experiments were carried out stepping the potential between 0.5 and 1.2 V and back, after a 2 min preconditioning at the initial potential. The solution of the cell is 0.01 M KCl, unless otherwise stated, and the pH was adjusted to 3 adding HCl. All potentials arte reported against the silver/silver chloride (Ag/AgCl) electrode. All measurements are made in air and no effect of nitrogen bubbling in the solution was observed.

2.8. Digital simulation

Digital simulation of cyclic voltammetric experiments was performed using the Electrochemical Simulation Package (ESP 2.1) a program written by Carlo Nervi [44]. The simulation were performed in a personal computer (Pentium III, 1 Gb RAM, 40 Gb hard disk) running DOS (inside a Windows XP environment). The simulated data points were then imported into Origin 7.0 (Microcal) for comparison with experimental data.

2.9. Semi-infinite boundary conditions

In Scheme 2a it is described the experimental set-up used to measure the electrochemistry of the loaded hydrogels. The thickness of the diffusion layer (δ) is related with the time of the measurement and the diffusion coefficient:

$$\delta = \sqrt{Dot} \quad (3)$$

Even at the longest time span used (300 s) and with a diffusion coefficient usual in a viscous media ($Do < 1 \times 10^{-6}\,cm^2\,s^{-1}$), the diffusion layer thickness is ca. 0.02 cm, which is smaller than the actual thickness of the polymer sample (0.3 cm). Therefore, the semi-infinite condition is fulfilled, which is not the case for the measurements using thin films of electroactive polymers deposited on the electrode, where a thickness below 3 μm is usually used (Scheme 2b).

Therefore, in the latter case short measurement time spans (< 100 ms) have to be used or systems having slow mass transport (denoted by small diffusion coefficients, $Do < 1 \times 10^{-7}\,cm\,s^{-1}$) can only be measured [45,46]. This is usually the case for compact polymers while it is unlikely to occur in porous polymer networks, like crosslinked hydrogels.

3. Results and Discussion

As it was discussed above, since the electroactive polymers are produced by loading tris(phenanthroline)iron(II) (TPFeII) inside different hydrogels: poly(2-acrylamidopropansulfonic acid) (PAMPS), poly(acrylic acid) (PAA) and the 1:1 copolymer:poly (acrylic acid-co-(2-acrylamidopropansulfonic acid)) (PAA-co-AMPS). Subsequently, the electroactive polymers are designed: TPFeII@PAMPS, TPFeII@PAA and TPFeII@PAA-co-AMPS. The conditions are chosen to maintain dilute solutions of the redox complex inside the hydrogels. The chemical structure of the hydrogel matrixes includes an ionomer (PAMPS), a polar neutral polymer (PAA) and the copolymer having both monomer units (PAA-co-AMPS). To assure that PAA is not ionized the pH is kept at 3, while the pKa of PAA is 4.6.

3.1. Physicochemical properties of the polymers

Fig. 1 shows the swelling kinetics of the different materials in 0.01 M KCl/H_2O. The swelling is usually measured in water but in our case we are interested to know the properties in the conditions where the electrochemical properties will be measured. As it can be seen, the hydrogels containing the anionic groups (-SO_3^-):

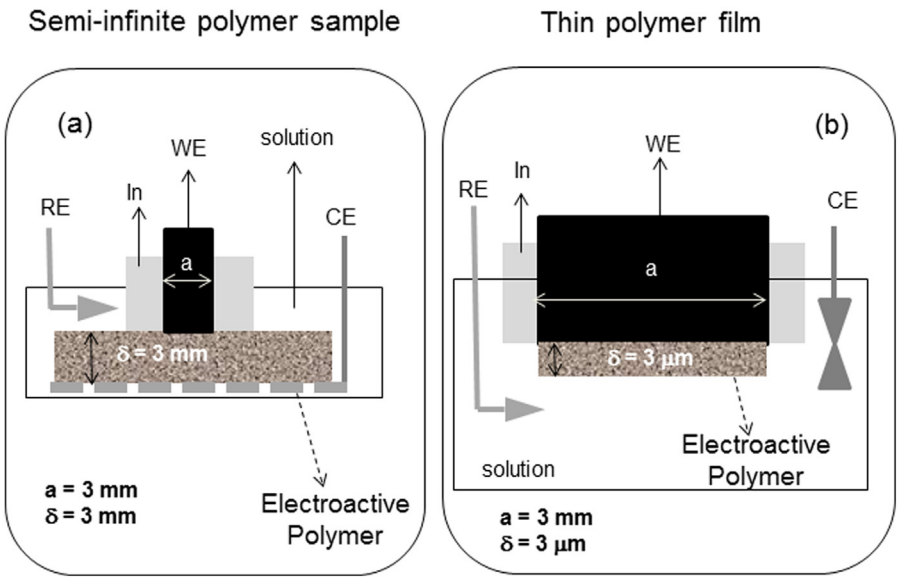

Scheme 2. Schematic of the measurement set-up for the electroactive hydrogels (a) compared with the usual deposited thin film on electrodes (b).

PAMPS and PAA-co-AMPS, show a fast and large swelling. This is due not only to high solvation of the polymer chains due to ion dipole interaction between the water molecules but predominantly to the osmotic effect of the mobile counterions (K^+) which are present to maintain electroneutrality and requires a large amount of solvent (water) to be solvated. On the other hand the polar neutral groups (at pH 3) in the acrylic acid (PAA) show a slow and small swelling. Besides the absence of charged groups and osmotic effect, it is likely for hydrogen bonds between neighboring —COOH groups to be present, a well-known effect in carboxylic acids [47].

It is noteworthy that both the swelling at equilibrium ($\%Sw_{eq}$) of the copolymer (PAA-co-50%AMPS) is larger than that of pure AA. This result suggests that the properties of the copolymer are not simple addition of the properties of each monomer unit.

The swelling of the hydrogel is a process where the solvation of the polymer chains is counterbalanced by the elastic constant of the crosslinked polymer matrix. The rate of swelling is related to the rate of relaxation of the polymer chains in the hydrogel matrix. Nonlinear fitting of the swelling curve with a first order kinetics equation [48]:

$$\%Sw(t) = \%Sw_{eq}(1 - e^{-Kst}) \quad (4)$$

where Ks is the rate constant of the pseudo-first-order swelling model. The values (Table 1) suggest that the hydrogel of PAA is significantly more rigid and having a slower relaxation than the others, while the faster to relax is PAMPS, showing the copolymer (PAA-co-AMPS) an intermediate value.

As it can be seen (Table 1) the partition coefficients of inside the hydrogels are quite large in all cases. The molar concentration does not directly scale up with the partition coefficient since they take into account the swelling of the hydrogel, which decreases the inner concentration.

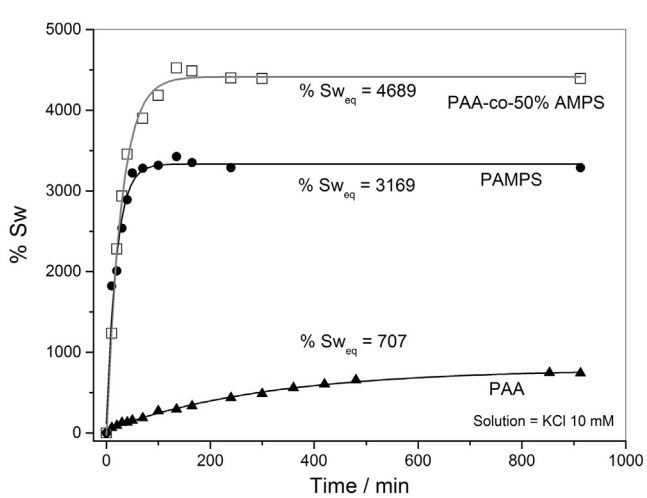

Fig. 1. Swelling kinetics of the hydrogels in 0.01 M KCl (pH = 3).

3.2. Electrochemical response of the electroactive polymers

3.2.1. Cyclic voltammetry of the redox complex in solution

The cyclic voltammetry of TPFeII in aqueous solution (Fig. 2) shows a quasireversible response. The peak currents (oxidation and reduction) show linear relationships with the square root of the scan rate ($v^{1/2}$) (see insert in Fig. 1). The results are in agreement with those reported before. [49–51].

The cyclic voltammetric responses of the different electroactive polymers made by loading TPFeII inside different hydrogels are shown in Fig. 3. In all cases, the current increases with the scan rate. The peak currents scale up with the square root of the scan rate, giving straight lines (see inserts in Fig. 3) suggesting a dominant diffusion control of the charge transport inside the films.

However, while TPFeII@PAMPS and TPFeII@PAA-co-AMPS show a nearly reversible voltammogram, the response of TPFeII@PAA show a large peak potential difference ($\Delta Ep = (Ep_{anodic} - Ep_{catodic}) > 59mV$) which means that charge transfer is slow. In all cases, when the scan rate (v) is increased, shifts of Epa and an increase in ΔEp are observed signaling the onset of effects of the heterogeneous electron transfer rate (k_o). Information about k_o can then be obtained from the variation of Epa or ΔEp with the scan rate but we will use digital simulation for that purpose (Section 3.3.3).

Moreover, the mass transfer parameters (diffusion coefficient) could also be estimated from the slopes of the peak current vs $v^{1/2}$ plots but the calculation should take into account the charge

Table 1
Physicochemical data of the different electroactive polymers[a].

Electroactive polymer	P_{molal}	Gel density ($g\,cm^{-3}$)[b]	c x 10^6 [$mol\,cm^{-3}$]	Sw_{eq}%	Swelling Rate constant (K_{sw}/s^{-1})
TPFeII@PAMPS	1725	0.954	12.2	3169	5.33×10^{-2}
TPFeII@PAA	244	1.128	51.9	707	3.80×10^{-3}
TPFeII@PAA-co-AMPS	1523	0.983	11.0	4689	3.58×10^{-2}

[a] All gels are equilibrated with 1 mM [$(Phen)_3Fe^{+2}$] in 10 mM KCl containing excess (0.1 mM) of added phenanthroline to avoid complex hydrolysis.
[b] the density was calculated using the volume measured by solution displacement in a graduated cylinder.

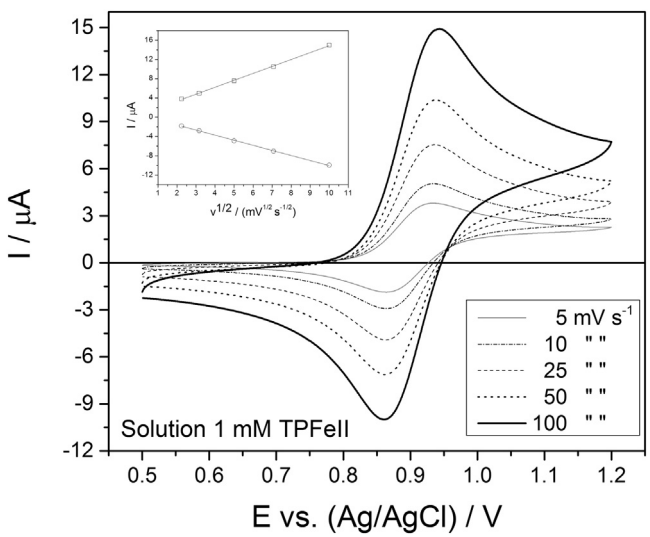

Fig. 2. Cyclic voltammograms of a glassy carbon electrode in a 1 mM solution of tris (phenanthroline)iron(II) in 0.01 M KCl.

transfer parameters which are unknown. Therefore, we used chronoamperometry at large enough potentials to assure fast charge transfer conditions (Section 3.3.1).

It is noteworthy that cyclic voltammetric responses of the electroactive polymer can be easily measured with a simple set-up and in the presence of a low electrolyte concentration. A low electrolyte concentration was used to maintain the hydrogel swelled and the redox probe at large enough concentration inside the hydrogel. Larger electrolyte concentrations induce the hydrogel volume to decrease due to the decreased availability of free water to solvate the hydrogel chains [52]. Additionally, the presence of mobile ions in the solution decrease the Donnan potential between the charged hydrogel and the external solution, lowering the driving force for retention of the redox complex.

The cyclic voltammetric responses seem to depend on the chemical composition of the hydrogels. Therefore, it is likely that both the heterogeneous charge transfer and the mass transport depend on the hydrogel matrix used to make the electroactive polymer.

3.3. Evaluation of mass transport inside the polymers

First, the diffusion coefficients are determines by chronoamperometry. Then, the hydrogel viscosities are calculated using Stokes-Einstein theory.

3.3.1. Chronoamperometric measurements

The chronoamperometric profile of TPFeII@PAMPS (Fig. 4a) shows a symmetric response during oxidation and reduction processes. The Cottrell's plots (*i(t)* vs $t^{-1/2}$) show linear relationships allowing to calculate the diffusion coefficient using Cottrell's equation [53]:

$$i(t) = \frac{nFAC\sqrt{D}}{\sqrt{\pi t}} \tag{5}$$

The chronoamperograms are symmetrical and the Cottrell's plots (*i* vs $t^{-1/2}$) are also linear ($R^2 > 0.99$) for all the other electroactive polymers studied. (Fig. S3, supplementary information). The values at short times ($t^{-1/2} > 0.8$) are not used to calculate the slopes since the current due to capacitive charging is present. Table 2 Therefore, Cottrell's equation is obeyed for all the electroactive polymers tested even for the slowest charge transfer (PAA) since a pulse potential large enough is used to assure complete conversion of the reduced complex at the electrode/polymer interface. The diffusion coefficients can be calculated from the slopes of the Cottrell's plots. The diffusion coefficient values (Table 2) are between 10^{-8} and $10^{-6}\,cm^2\,s^{-1}$ suggesting a relatively hindered mass transport of the complex inside the hydrogel. The diffusion coefficients and the ratio (D_{ox}/D_{red}) are similar to those reported for the same complex in ionic liquids [54], except for the case of the PAA based polymer. In the electroactive polymers including AMPS monomer unit, the larger value is observed in the homopolymer, with 100% anionic groups compared with the copolymer, with only 50% of anionic groups.

In the case of PAA based polymer, the ratio is inverted being the diffusion coefficient of Fe(phenanthroline)$_3^{3+}$ larger than Fe (phenanthroline)$_3^{2+}$. It is unlikely that the effect is physically inverted in a neutral polymer. On the other hand, in a neutral matrix migration effects can be dominant. The derivation of Cottrell's equation assumes that the mass transport of the electroactive species is solely controlled by diffusion, since a large amount of non electroactive and mobile inert electrolyte, usually called supporting electrolyte, is present. Inside a neutral hydrogel (e.g. PAA) such a condition could not be fulfilled since there are no mobile ions besides TPFeII and its counterion. On the other hand, it has been shown that Cottrell's equation still holds when redox ions are driven both by migration and diffusion [55,56]. Lange and Doblhofer simulated the chronoamperometric profiles due to the mass transport of redox charged species inside membrane-type polymers, using the complete Nernst-Planck equation [57]. The measured diffusion coefficient differs from the one which would be measured in the presence of excess supporting electrolyte.

Using the correction factor described by Lange and Doblhofer, it is possible to calculate the correction factor, which is a function of the ratio (D_{Ox}/D_{Red}) [57], and the charge difference ($z_{Red} = 2$ and $z_{Ox} = 3$). Using a ratio $D_{Ox}/D_{Red} = 0.74$ (the one measured in solution), the correction factor are calculated [57]. Therefore, the ratio becomes closer to those observed in the other electroactive polymers(Table 2).

The chronoamperometry in solution also renders a linear Cottrell plot. The value of the diffusion coefficient in solution is $D = 9.0(\pm 0.5)$ x $10^{-6}\,cm^2 \cdot s^{-1}$. The later value is close to that measured by Bard and coworkers by cyclic voltammetry ($D = 4.9$ (± 0.5) x $10^{-6}\,cm^2 \cdot s^{-1}$) [58].

The last two columns in Table 2 show the calculated thickness of the diffusion layer (Eq. 3), using the maximum time span (300 s)

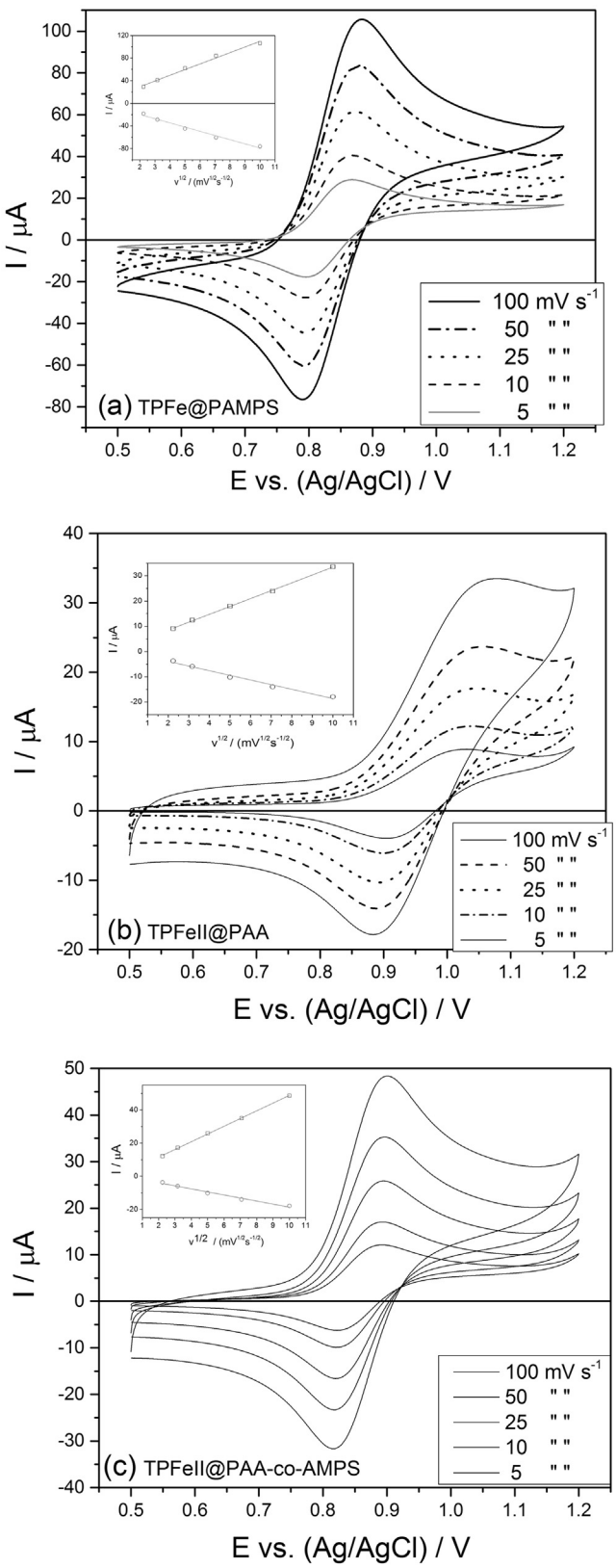

Fig. 3. Cyclic voltammetry of the different electroactive polymers: a) TPFeII@-PAMPS; b) TPFeII@PAA; c) TPFeII@PAA-co-PAMPS. Experimental parameters: T = 25 °C. A = 0.071 cm^2. External solution = 10 mM KCl (pH = 3).

and the actual thickness of the layer. As it can be seen the thickness of the polymer samples used in this work are at least 10 times larger than the calculated diffusion layer assuring that semi-infinite conditions are fulfilled. On the other hand, the thickness of the thin films used in previous work (ref in Table 2) is much smaller than the calculated diffusion layer making necessary to use short times (or fast scan rates in cyclic voltammetry) for the determination of diffusion coefficients.

The concentration of redox species could affect the measured diffusion coefficients. Oyama et al. [59], measured the diffusion coefficient of redox anions in protonated polyvinylpyrrolidone at different concentrations. They find out a strong effect of the concentration and only become constant at large (near 1 M) inner concentration. They attributed such effect to the chemical crosslink of the polymer chains by the multiply charged anions. In macroscopic hydrogels such effect will induce a decrease of the gel sample. In our case, we immerse the PAMPS hydrogel in different concentrations of the redox complex (0.5, 1, 5 and 10 mM). No noticeable volume change was observed when the hydrogels is immersed in solution 0.5 or 1 mM in TPFeII while clear volume changes are observed for concentrations larger than 1 mM (Fig. S6. supl info). The likely reason is a change of density due to ionic crosslinking of the anionic polymer chains by the divalent cation (TPFeII) [60]. Therefore, no attempt was made to determine mass transport in collapsed gels, which were immersed in TPFeII solutions at c > 1 mM. On the other hand, the diffusion coefficient was determined with the electroactive polymer made using a 0.5 mM TPFeII loading solution. The measured D is ion agreement with the data reported in Table 2 for PAMPS.

3.3.2. Calculation of the viscosity using the diffusion coefficient of a redox probe

In a homogenous media, the diffusion coefficient is directly related to the viscous properties of the media. Einstein [61] derived from the Navier–Stokes differential equations for a sphere moving in a viscous medium an expression for the diffusion coefficient D for such spheres that may be rewritten as:

$$D = \frac{kT}{6\pi r_{ion}\eta} \tag{6}$$

where k is the Boltzmann constant, T the temperature, r_{ion} is the radius of the solvated ion and η the viscosity of the medium.

From Eq. 6 can be deduced that, assuming that the ion dimension is the same in different solvents (r_{ion} is unchanged), the product of the viscosity (η) and the diffusion coefficient (D) of the ion is the same, irrespective of the media:

$$\eta_w D_w = \eta_m D_m \tag{7}$$

where the subscript w denotes the value measured in water and the subscript m the values measured in another media.

Eq. 7 is equivalent to the Walden's rule for ion mobilities and it has been used to calculate the diffusion coefficient of a redox probe in a solvent of known viscosity, using the diffusion coefficient and viscosity in water [24]. The redox probe used (TPFeII) is a large ion and it is unlikely for he solvation sphere to change in different media. Therefore, r_{ion} can be assumed constant and Eqs. (6) and (7) to be obeyed. In our case, we use it to calculate the unknown viscosity of the hydrogel. The data are depicted in Table 2. The calculated viscosities from the oxidation and reduction differ for less than 8% between them. This low dispersion between the independent values suggests that the calculated value reflect the viscosity of the hydrogel media.

The calculated viscosity of PAA is ca. 10 times larger than that of PAMPS, while PAA-co-PAMPS show an intermediate value. The viscosity values are in the order of those calculated, using the same procedure and the data described in Ref. [24], for related ionomers (Nafion® and poly(stryenesulfonate (PSS)) (Table 2). As it can be seen, Nafion® shows a viscosity much larger than PSS likely due to

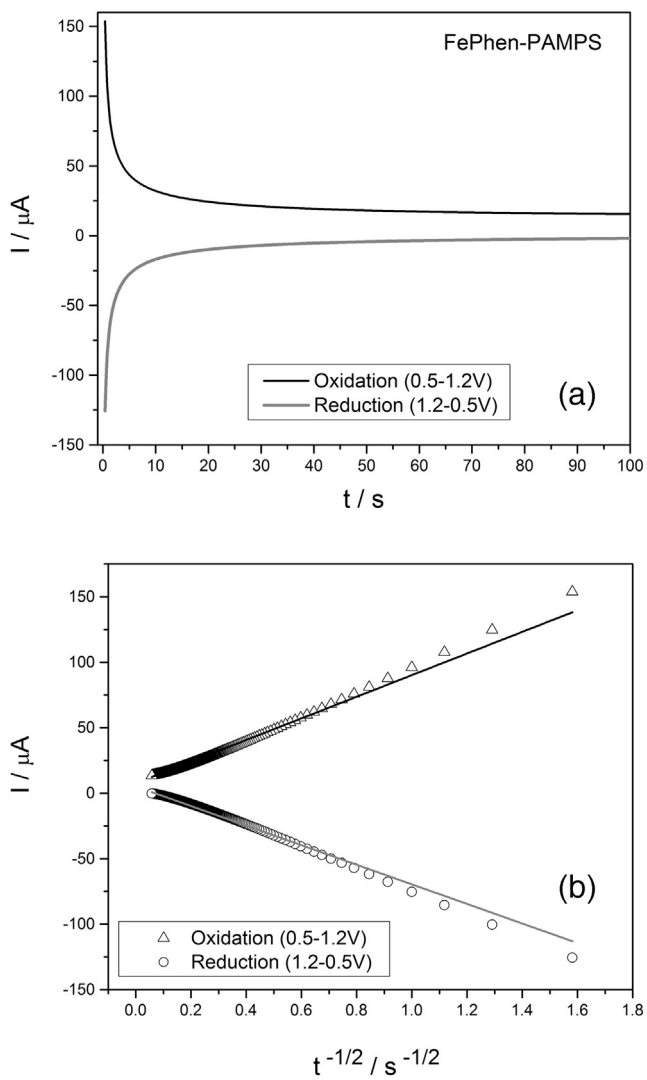

Fig. 4. (a) Chronoamperometric plots for TPFeII@PAMPS. (b) Both anodic (0.5 to 1.2 V) and cathodic (1.2 to 0.5 V) excursion are shown. (c) Cottrell's plots for TPFeII@PAMPS. Both anodic (0.5 to 1.2 V) and cathodic (1.2 to 0.5 V) excursion are shown.

lower swelling. This is reasonable since Nafion® contains hydrophobic domains which make it insoluble in water while PSS is highly soluble in water and the diffusion coefficient of the redox probe ($Ru(bpy)_3^{2+}$) inside the film has to be measured in a methanol/acetonitrile mixture [62]. While viscosity values larger than 100 cP are unusual in aqueous solution, such values have been measured in ionic liquids [63].

The calculated viscosity coefficients of the redox species correlate with the swelling rate (K_{sw}, Table 1) which is related to the elasticity of the hydrogel (Fig. 5). The largest viscosity is measured for PAA which shows the smallest swelling rate constant (K_{sw}).

3.3.3. Digital simulation for evaluation of electrochemical parameters

Digital simulations of the linear sweep voltammetry responses were performed using an electrochemical simulation package (see experimental part). As it can be seen, (Fig. 6) good fitting was obtained for all the hydrogel materials. The obtained charge transfer constants (Table 3) depend on the chemical structure of the hydrogel. The electrode potential is also affected by the hydrogel where the redox complex is sorbed. Azad et al [64], has proposed that the anionic nature of the polymer matrix (Nafion® in their work) decrease the redox potentials of different iron complexes (including TPFeII), compared with solution, through a better stabilization of the more cationic iron(III) species. In this work, we observe lower redox potentials for TPFeII@PAMPS and TPFeII@PAA-co-PAMPS than those measured for TPFeII in solution. It is likely that in both cases the more cationic Fe(III) species is more stabilized than the Fe(II) species. On the other hand, the redox potential of TPFeII@PAA is more positive than the one measured in solution. In this case, the absence of fixed counterions makes the more cationic Fe(III) species less stabilized and the redox potential shifts to more anodic values.

The charge transfer constant measured for TPFeII in solution ($0.05\ cm{\cdot}s^{-1}$) is similar to those previously reported ($0.058\ cm{\cdot}s^{-1}$) [49].

As it can be seen, the heterogeneous charge transfer of the redox complex inside the polymer is clearly affected by the polymeric environment. The charge transfer of the redox complex in TPFeII@PAMPS is similar to that in solution. On the other hand, the charge transfer constant in TPFeII@PAA is 100 times smaller. Finally, the charge transfer in the loaded copolymer (TPFeII@PAA-co-PAMPS) is only slightly smaller than in solution.

While it could be envisaged that the charge transfer constant of an outer sphere redox couple, like TPFeII should be unaffected by the presence of the hydrogel, previous results loaded ionomers with similar redox probes show that heterogeneous charge transfer rates are usually lower inside the polymer than in solution [65,66]. These results has been explained taking into account the effect of solvent viscosity on the local reordering during the charge transfer [67]. One possible way to explain the observed relationship between the charge transfer constant (k_o) and the viscosity (η) imply the application of Marcus theory for an outer sphere electrons transfer [68]. For an adiabatic electron transfer reaction that involves predominantly solvent reorganization, the standard free energy of activation the frequency of attempts on the energy barrier is proportional to the longitudinal relaxation time of the solvent (τ_l). Following the discussion by Bond and coworkers [63], the logarithm of the charge transfer constant ($\ln(k_o)$) could be expressed as:

$$\ln(k_0) = [\ln(Ap) - \frac{\Delta G^{\dagger}}{RT}] - \theta \ln(\tau_l) \quad (8)$$

where Ap is the pre-exponential factor of the charge transfer kinetics, ΔG is the free energy of activation and θ is a fraction between 0 and 1 which defines how adiabatic is the process (1 being the maximum adiabaticity).

The phenomenon is known as solvent dynamics effect [63]. The formalism has been used previously to explain the dependence of k_o on the solvent viscosity [69,70].

τ_l is proportional to the local viscosity, and can be calculated using eq. (9):

$$\tau_l = 3V_m(\varepsilon_\infty/\varepsilon_0)\eta/RT \quad (9)$$

where V_m is the molar volume of the medium, ε_∞ and ε_o are the high frequency and static permitivities.

Combining Eqs. (8) and (9) gives:

$$\ln(k_0) = [\ln(Ap) - \frac{\Delta G^{\dagger}}{RT}] - \theta \ln(3V_m(\varepsilon_\infty/\varepsilon_0)\eta/RT) - \theta \ln(\eta) \quad (10)$$

Since the first two terms does not depend on the viscosity, agreement with the model will be represented by a linear relationship between $\ln(k_o)$ and $\ln(\eta)$ with a slope **-θ**.

Using the viscosities calculated from the diffusion coefficients and the k_o values calculated from the simulation of the cyclic voltammograms, a plot can be drawn (Fig. 7). As it can be seen, the data fits a straight line with slope = −1 suggesting that the data are

Table 2
Diffusion coefficients of the TPFeII inside of the different electroactive polymers.

Hydrogel Matrix	D x 10^6/cm^2 s^{-1} (std. error) Oxidation	Reduction	Ratio (D^{3+}/D^{2+})	Viscosity[b] mPa s	Diffusion layer thickness[e] cm	Layer thickness cm
PAMPS	3.0 (±0.2)	2.5 (±0.2)	0.82	2.53 (±0.2)	0.030	0.3
PAA	0.024 (±0.002) 0.033[a] (±0.002)	0.034 (±0.002) 0.024[a] (±0.002)	1.43 0.73[a]	245[a] (±4)	0.031[a]	0.3
PAA-co-AMPS	0.70 (±0.02)	0.56 (+/−0.02)	0.80	11.0 (±0.6)	0.014	0.3
Solution	9.0 (±0.2)	6.7 (±0.2)	0.74	0.890[c]	0.051	3
Nafion®	0.0214[c] (±0.0008)	–		31.1[d]	0.0025	0.00016[c]
PSS	0.146[c] (±0.008)	–		212.1[d]	0.0066	0.00001[c]

[a] calculated considering migration effects.
[b] calculated using Walden's rule. The value reported is the arithmetic mean for the oxidation and reduction process and the error the standard deviation of the mean.
[c] data from *Knoche KL*, et al., *J. Electrochem. Soc., 160(2013)H285-H293* with $Ru(bpy)_3^{2+}$ as redox probe.
[d] calculated using Eq. (6).
[e] calculated from the largest value of the diffusion coefficient using a time span of 300 s.

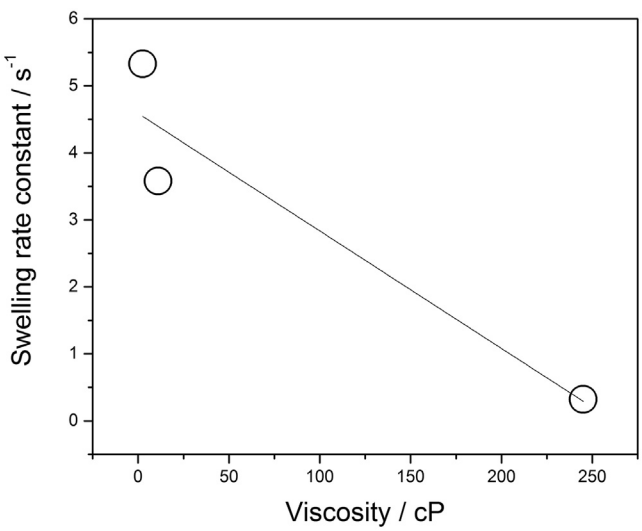

Fig. 5. Relationship between calculated viscosity and the swelling rate constants (K_{sw}) for the different hydrogels studied.

in agreement with the model with a strongly adiabatic reaction. The relationship has been found to be obeyed in a eleven fold range of the parameters [71], and has been observed in viscous liquid media [72–74], and for homogeneous charge transfer [63].

Since the viscosity is calculated from the measured diffusion coefficients while the charge transfer constant is measured independently by simulation of the cyclic voltammograms, the good fitting (R^2 = 0.93) suggests that modeling the hydrogels as viscous fluids which control locally (at the interface) the charge transfer and at longer ranges (diffusion layer) the mass transport is adequate.

The fabrication of electroactive polymers by loading the same redox couple in chemically related polymeric hydrogel matrixes allows measuring such correlations. Additionally, the observed effect confirms a close contact of the electrode with the polymer. If a thin layer of solution is trapped between the gel and the electrode, the diffusion coefficients will still be those of the hydrogels because the diffusion layer develops into the hydrogel at long times. However, the effect of viscosity on the charge transfer is a local phenomenon which could only occur if the viscous solvent is present on the site of the charge transfer.

The partition equilibrium of the redox complex between the hydrogel and the solution is set by the relative interaction between the hydrogel chains and the solvation in water. In an ionomer (e.g. PAMPS) the dominant interaction is electrostatic between the negative fixed groups ($-SO_3^-$) and positive redox complex (TPFeII). However, there is a site competition between the electroactive cations and the cations of the electrolyte. We have used a low electrolyte concentration to avoid decreasing the redox complex concentration inside the hydrogel to test the relevancy of this effect we measure the electrochemical response of electroactive polymers made by loading TPFeII ions from 1 mM solutions and varying electrolyte (KCl) concentrations. The results (Fig. S3, supplementary information) show that the currents decrease when the electrolyte concentration increases while the voltammetry shape response remains almost unchanged. It is likely that the inner concentration of the redox complex decreases when the total ionic force is increased. Indeed, the partition coefficient (P_{molal}) of TPFeII in PAMPS is 0.72 times smaller (1069) when 30 mM KCl is used as electrolyte than the one measured with 10 mM KCl electrolyte.

All cyclic voltammograms responses show peak current in the same range (10–100 μA at a scan rate of 50 mV s^{-1}) values for different parameters (concentration, diffusion coefficient, charge transfer constants). The good fitting of simulated values, using the concentration measured independently, the diffusion coefficients measured by chronoamperometry and only adjusting the charge transfer parameters, suggests that those parameters represent adequately the experimental measurements. Moreover, the diffusion coefficients recovered from the peak current vs square root of scan rate plots are in the order of more precise values measured by chronoamperometry measurements.

3.4. Loading redox active ions inside hydrogels bearing the same charge

The hydrogel matrix and the bathing solution could be considered separate phases. If the hydrogel contains permanently charged groups (e.g. $-SO_3^-$ in PAMPS) an ionic equilibrium is

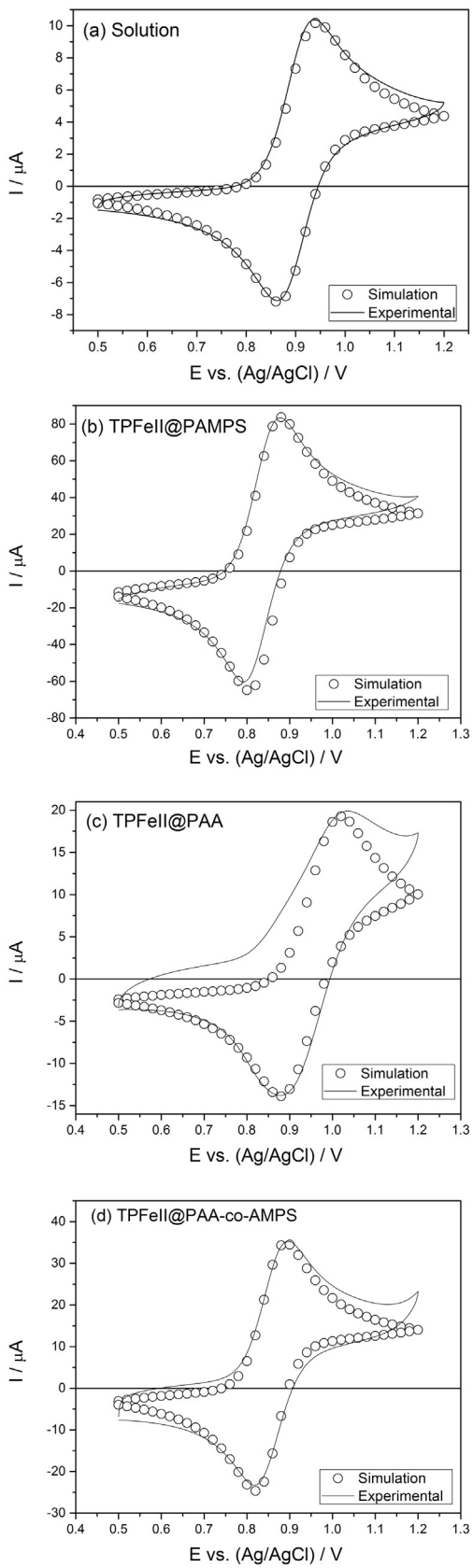

Fig. 6. Digital simulation of the linear sweep voltammetry responses using the following parameters: (a) Solution of TPFeII: ke = 0.05 cm·s^{-1}, E = 0.900 $V_{Ag/AgCl}$, C = 1 mM, D_{Red} = 9 × 10^{-6} cm^2/s, D_{Ox} = 6.7 10^{-6} cm^2·s^{-1}, α = 0.5. (b) TPFeII@PAMPS: ke = 1 × 10^{-2} cm·s^{-1}, Eo = 0.840 $V_{Ag/AgCl}$, C = 12.20, D_{Red} = 3.0 × 10^{-6} cm^2·s^{-1}, D_{Ox} = 2.5 10^{-6} cm^2/s, α = 0.5. (c) TPFeII@PAA: ke = 1 × 10^{-4} cm·s^{-1}, Eo = 0.940 $V_{Ag/AgCl}$, C = 51.9, D_{Red} = 3.3 × 10^{-8} cm^2·s^{-1}, D_{Ox} = 2.4 10^{-8} cm^2·s^{-1}, α = 0.5. (d) TPFeII@PAA-co-PAMPS: ke = 8 × 10^{-3} cm·s^{-1}, Eo = 0.850 $V_{Ag/AgCl}$, C = 11.0, D_{Red} = 7.0 × 10^{-7} cm^2/s, D_{Ox} = 5.6 × 10^{-7} cm^2·s^{-1}, α = 0.5. All cyclic voltammograms were measured using a scan rate of 50 mV·s^{-1}. The experimental response is shown as full lines while the open circles show the simulated cyclic voltammograms.

established where mobile counterions (e.g. K^+) are taken from the solution and mobile anions (e.g. Cl^-) are excluded. In that sense, the electrochemical currents due to redox active anions could not be measured inside PAPMS because the anions are not present. As it has been shown above electroactive cations are absorbed inside negatively charged hydrogels. However, the largest concentration inside the hydrogel sample is achieved using a neutral polymer matrix (PAA) suggesting a large effect of hydrophobic interactions on the partition coefficient [75]. Szentirmay and Martin, show that large complexes with organic ligands (e.g. $Ru(bpy)_3^{2+}$) are strongly absorbed inside a negatively charge ionomer (Nafion®) while smaller complexes with inorganic ligands (e.g. $Ru(NH_3)_6^{2+}$) absorb weakly and Fe^{+2} is not retained [76]. To ascertain the extent of the effect we measured the redox response of different redox active anions.

3.4.1. Fabrication of an electroactive polymer by loading ferrocyanide ions inside PAMPS

Being a model redox compound in electrochemistry, ferrocyanide/ferricyanide redox couple ($Fe(CN)_6^{-4}/Fe(CN)_6^{-3}$) has been used to build electroactive polymers by loading inside thin films of ionomers bearing positive charges [77–80] such as quaternized poly(vinylpyridine) [81,82]. On the other hand, it is known that ferricyanide can diffuse trough negatively charged ionomers (e.g. Nafion® [83]) or neutral hydrogels. [84]. Moreover, it has been shown that ferricyanide can be oxidized on glassy carbon after diffusion trough a thin film of Nafion® [85]. The sorption of ferricyanide inside a negatively charged hydrogel (PAMPS) was tried by immersing the hydrogel in 10 mM solution of potassium ferricyanide for 48 h. The hydrogel was then studied by cyclic voltammetry (Fig. 8).

As it can be seen, a clear electrochemical response is observed. The peak potential difference is close to 59 mV, suggesting fast charge transfer. The redox potential is in agreement with the one reported before for ferricyanide in low concentration electrolyte (0.1 M KCl) [53]. Moreover, the peak currents depend linearly on the square root of the scan rate, suggesting mass transport control. It is noteworthy that, unlike the response observed with a thin film Nafion® covering the electrode [84], the bathing solution contains only 10 mM KCl. Therefore, the current signal could not be due to ferrocyanide ion transported from the solution through the film but is due to ferrocyanide ions retained inside the hydrogel. Moreover, we measure a typical response for a semi-infinite diffusion of a reversible couple while in Ref. [73] a nearly sigmoidal response was obtained. Multicharged coions (e.g. $Fe(CN)_6^{-3}$) of the fixed groups in PAMPS ($-SO_3^-$) should be destabilized by columbic interactions. However, it seems that ferrocyanide ions are hydrophobic enough to overcome charge repulsion and be loaded inside the anionic polymer. The observed loading seems to be a novel way to produce electroactive polymers by loading redox ions inside hydrogels of the same charge.

3.4.2. Simultaneous absorption of redox anions (nitrite) and cations (TPFeII) inside PAMPS hydrogel

Since tris(phenanthroline)iron(II))/(III) couple has a redox potential of ca. 1.060 V vs SHE [86], it is able to oxidize homogeneously different chemical substances (e.g. nitrite ion) which are difficult to oxidized electrochemically on bare electrodes due to a slow charge transfer on glassy carbon [87]. Indeed, TPFeII adsorbed on bentonite [88], and the related couple: $Fe(bipyridil)_3^2$

Table 3
Electrochemical parameters for the different electroactive polymers and aqueous solution used to simulate the measured cyclic voltammograms.

System	E_{app}[a] vs. (Ag/AgCl) (V)	k_0 ($cm\,s^{-1}$)
TPFeII@PAMPS	0.84	0.01
TPFeII@PAA	0.94	0.0001
TPFeII@PAA-co-AMPS	0.85	0.008
TPFeII Solution	0.90	0.05

[a] Standard potential used in the simulation.

$^{+/3+}$ loaded inside Nafion® [73], have been used to oxidize electrochemically nitrite with analytical purposes. In the latter case [73], the catalytic redox complex is loaded inside a thin film of a ionomer (Nafion®). Nitrite ions are present in solution and could be electrochemically oxidized at the film surface. However, in more recent work, Azad et al. find that the anions (nitrite, arsenite) indeed ingress into the thin film and react close to the substrate electrode [62]. They suggest that the presence of large redox cations promote the anion transport inside the anionic ionomer. On the other hand, anion rejection by thin films of an anionic polymer (Nafion®) has been shown [89].

In our case, the bathing solution only contains 10 mM KCl and the nitrite which is oxidized is previously loaded. Coions (e.g. NO_2^-) of the fixed groups in PAMPS ($-SO_3^-$) could not be stabilized by electrostatic interactions. However, it seems that nitrite ions are hydrophobic enough to overcome charge repulsion and be loaded inside the anionic polymer [90].

In our electroactive polymers, the polymer/solution interface is inaccessible during the electrochemical experiment. However, a clear signal due to the oxidation of nitrite is observed, (Fig. 9) while no signal is detected in the same conditions in the absence of tris (phenanthroline)iron(II/III) ($Fe(phen)_3^{2+}/Fe(phen)_3^{3+}$. The reaction follows a electrochemical-chemical mechanism [65]:

4 $Fe(phenanthroline)_3^{2+} = 2\ Fe(phenanthroline)_3^{3+} + 2\,e^-$ Electrochemical (I)

2 $Fe(phenanthroline)_3^{3+} + NO_2^- + H_2O = 2\ Fe(phenanthroline)_3^{2+} + NO_3^- + 2\,H^+$ Chemical (II)

The redox complex is electrochemically oxidized (I), and the following chemical reaction (II) regenerates the reduced complex which then reoxidized electrochemically by reaction (I). The kinetic parameters can be calculated by digital simulation of the voltammetric response (Fig. S4, supl information).

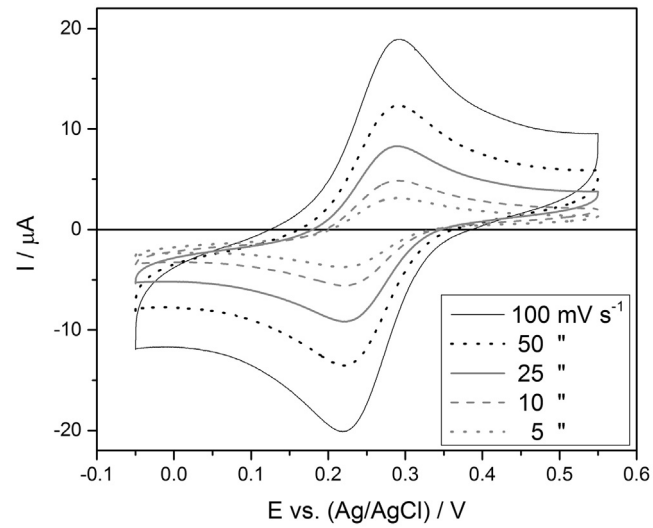

Fig. 8. Cyclic voltammograms of glassy carbon electrode in a electroactive polymer made by loading ferricyanide ($Fe(CN)_6^{-3}$), from a 10 mM solution, inside a PAMPS hydrogel. Electrolyte solution = 10 mM KCl. A = 0.071 cm^2.

The rate constant (k_f) of the chemical process is quite large ($50\,s^{-1}$) suggesting that TPFeII@PAMPS is a good catalytic system to oxidize electrochemically nitrite. However, as it was observed before for the $E_{qrev}C$ reaction of Fe^{2+} catalyzed by TPFeII loaded inside a poly(acrylamide-co-(2-acrylamidosulfonic acid) hydrogel [43], the charge transfer constant ($k_o = 2 \times 10^{-5}$ $cm\,s^{-1}$) is much smaller than the value observed for TPFeII@PAMPS alone ($k_o = 0.01$ $cm\,s^{-1}$).

While several authors [73,77,91], have used the redox catalysis by immobilized redox couples of ions (e.g. nitrite, arsenite) for direct analytical detection of the ion sin solution, our system is unlikely to be used for such purpose since long (24–48 h) loading times of the analyte are required due to the large thickness of the hydrogel samples. On the other hand, the observed catalysis reveals a new method to perform complex electrochemical (and/or chemical) reactions inside hydrogel matrixes. Since ions of different charges could be loaded inside charged or neutral

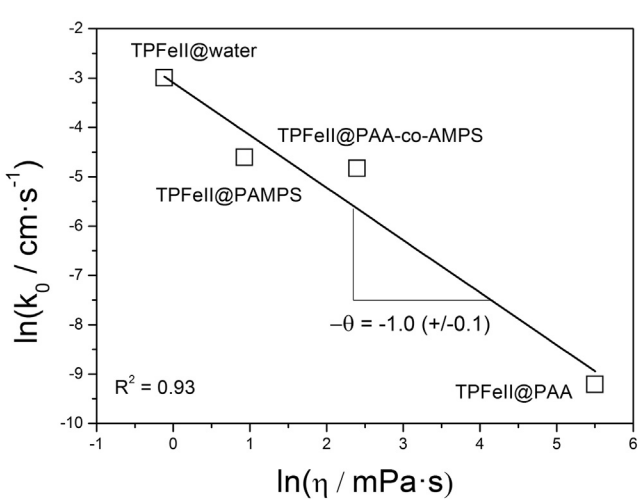

Fig. 7. Relationship between the heterogeneous charge transfer constant (k_o) and the viscosity (η) for the different media studied.

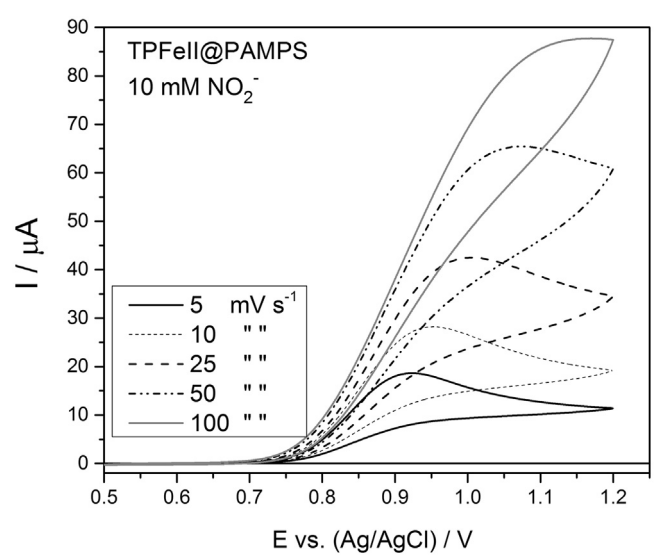

Fig. 9. Cyclic voltammograms of an electroactive polymer (TPFeII@PAMPS) loaded with 10 mM nitrite, at different scan rates. A = 0.071 cm^2.

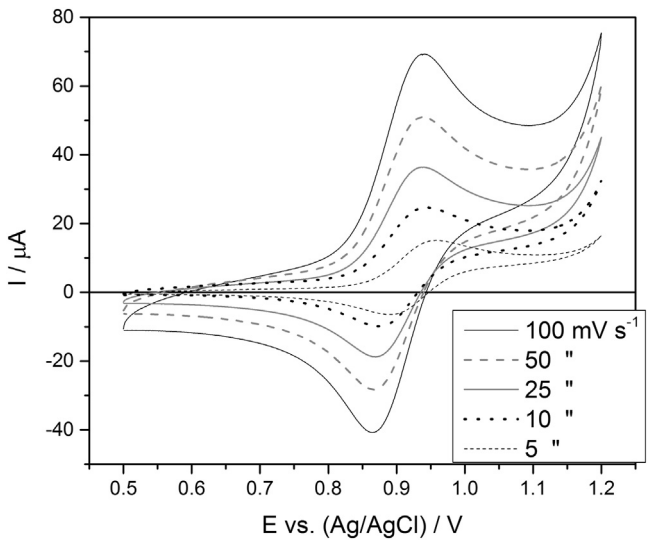

Fig. 10. Cyclic voltammograms of a glassy carbon electrode on an electroactive polymer (TPFeII@PAPMTAC) made by loading tris(phennathroline)iron(II) inside a (poly((3-acrylamidopropyl)trimethylammonium chloride), PAPMTAC) hydrogel. Electrolyte solution = 10 mM KCl. A = 0.071 cm^2.

hydrogels, seems that there are no limitations on the reactants to be used in more complex reactions.

3.4.3. Fabrication of an electroactive polymer by loading TPFeII inside a cationic hydrogel

It has been shown above that it is possible to measure the electrochemical properties of loaded negatively charged or neutral hydrogels by redox cations and anionic hydrogel by redox anions. The loading is possible due to the presence of hydrophobic interactions which overcome charge repulsion. A reasonable corollary is that a redox cation should be able to be loaded, in an electroactive form, inside a positively charged (cationic) hydrogel. Therefore, we tested the loading of a redox cations (TPFeII) inside a cationic hydrogel (poly((3-acrylamidopropyl) trimethylammonium chloride), PAPMTAC). In Fig. 10 it can be seen the cyclic voltammograms of a glassy carbon electrode pressed on an electroactive polymer made by loading TPFeII inside PAPMTAC. As it can be seen, a clear electrochemical response is measured. The peak potential differences are in the range 60–70 mV suggesting a quasi-reversible charge transfer. The peak currents increase linearly with the square root of the scan rates, suggesting semi-infinite diffusion as mass transport mechanism. The results show that it is also possible to make electroactive polymers by loading electroactive cations inside a cationic hydrogel.

4. Conclusions

A simple electrochemical set-up allows to study the electrochemistry of electroactive polymers made by loading a redox complexes (tris(phenanthroline)iron(II), TPFeII) inside polymeric crosslinked hydrogels. It is shown that a redox cation (TPFeII) can be loaded not only in anionic ionomers (e.g. poly(2-acrlyamidopropansulfonic) acid, PAMPS) but also inside polar uncharged hydrogels (e.g. poly(acrylic acid, PAA)). Both mass transport (diffusion coefficient) and charge transfer (heterogeneous rate constant) are affected by the hydrogel physicochemical properties. The latter are determined by measuring the swelling kinetics in the same electrolyte solution used during the electrochemical experiments. Two homopolymers: poly(2-acrylamidopropansulfonic) acid and poly(acrylic) acid and the 1:1 copolymer (PAA-co-AMPS) are synthesized and studied. The diffusion coefficients of the loaded redox specie (TPFeII) correlate well with the swelling rate which is related to the viscosity of the hydrogels. Using Stokes-Einstein formalism, the viscosity of the hydrogel could be calculated by relating the diffusion coefficient of the same redox probe in water and inside the hydrogel,

The heterogeneous charge transfer is also affected by the polymeric environment. While the charge transfer of TPFeII@-PAMPS is nearly as fast as in solution, the charge transfer constant of TPFeII@PAA is 100 times smaller. On the other hand, the charge transfer constant of TPFeII in the copolymer (PAA-co-PAMPS)) is somewhat smaller than in PAMPS. The results are discussed in the framework of Marcus theory considering that solvent reorganization during charge transfer is related to the local viscosity of the media. It is shown that the heterogeneous charge transfer constant depends on the inverse of the viscosity. The correlation between electrode charge transfer and mass transport, measured independently, support the assumption of a close contact between the electrode and the hydrogel media.

A redox anion (ferricyanide) was also loaded inside and anionic hydrogel (PAMPS) and a clear electrochemical response is observed suggesting that electroactive polymers can be produced by loading ions inside a hydrogel matrix of the same charge. Indeed, the oxidized form of the electroactive polymers oxidizes nitrite ions loaded inside the hydrogel. Even that a negatively charged ionomer (PAMPS) is used to produce the electroactive polymer, the nitrite ion is successfully loaded and oxidized. Moreover, it suggests that more complex electrochemical-chemical reactions can be performed inside the polymer matrix in a similar way to liquid solutions, irrespective of the charge of the reactants and polymer

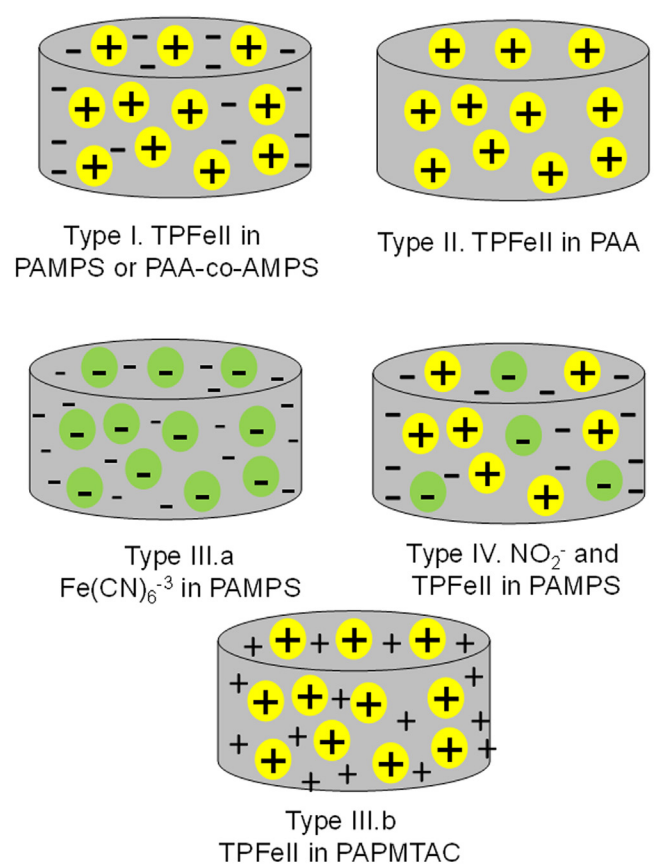

Scheme 3. Different kinds of electroactive polymers studied.

matrix. Additionally, it is shown that TPFeII cations are loaded inside a cationic hydrogel (PAPMTAC). The redox ion shows a quasi-reversible electrochemical response.

The results suggest that different kind of redox species (anionic or cationic) could be loaded inside any kind of hydrogels (cationic, anionic or neutral) to form electroactive polymers even when the hydrogel bear the same charge or no charge at all (Scheme 3). Type I is the usual ionomer [1], bearing fixed charges(negative here) loaded with redox ions of the opposite charge (positive here). Type II involves a neutral hydrogel loaded with redox ions (positive in this case). Type III is made by loading a negative redox ion inside an anionic hydrogel (III.a) or loading a positive redox ion inside a cationic hydrogel (III.b). Type IV is made by loading two redox ions of different charge (negative and positive) inside an ionomer (anionic in our work).

Since it has been shown [41], that it is also possible to load neutral redox couples (e.g. riboflavin) inside neutral hydrogels, it is likely that electroactive polymers could also be produced by loading neutral redox species inside charged (negative or positive) or neutral hydrogel matrixes.

The loading of redox ions inside bulk hydrogels seems to be a versatile method to produce model electroactive polymers which fulfill the semi-infinite boundary condition and the dilute solution thermodynamic approximation. It is noteworthy that the later approximation cannot be fulfilled with polymers containing covalently linked redox groups since large enough concentrations are required to allow for charge transport across the polymer by electron hoping between neighboring redox centers.

Acknowledgements

M.M. Bruno and C.A. Barbero, are permanent research fellows of CONICET. M.V. Martinez thanks CONICET for a graduate fellowship. The funding of CONICET and SPU are gratefully acknowledged. Prof. Carlo Nervi is gratefully acknowledged for the use of ESP 2.0.

Appendix A. Supplementary data

Supplementary data associated with this article can be found, in the online version, at http://dx.doi.org/10.1016/j.electacta.2016.10.007.

References

[1] Electroactive polymer electrochemistry, Part 1, Fundamentals, in: M.E.G. Lyons (Ed.), Springer, New York, 1994.
[2] Electroactive Polymer Electrochemistry, Part 2: Methods and Applications, in: M.E.G. Lyons (Ed.), Springer, New York, 1996.
[3] Electroactive polymer electrochemistry, Part 1, Fundamentals, in: M.E.G. Lyons (Ed.), Springer, New York, 1994, pp. 4.
[4] C.E.D. Chidsey, R.W. Murray, Redox capacity and direct current electron conductivity in electroactive materials, J. Phys. Chem. 90 (1986) 1479–1484.
[5] C.R. Martin, I. Rubinstein, A.J. Bard, Polymer films on electrodes. 9. Electron and mass transfer in Nafion films containing tris(2,2'-bipyridine)ruthenium(2 +), J. Am. Chem. Soc. 104 (1982) 482–4817.
[6] K. Sumi, F.C. Anson, Electron Transfer to Anionic Reactants Incorporated within Polycationic Coatings on Glassy Carbon Electrodes. Comparison of Random and Block Copolymers, J. Phys. Chem. 90 (1986) 3845–3850.
[7] D.A. Buttry, F.C. Anson, Effects of electron exchange and single-file diffusion on charge propagation in Nafion films containing redox couples, J Am Chem Soc 105 (1983) 685–689.
[8] S.W. Feldberg, Reinterpretation of polypyrrole electrochemistry. Consideration of capacitive currents in redox switching of conducting polymers, J. Am. Chem. Soc. 106 (1984) 4671–4674.
[9] C. Barbero, M.C. Miras, E.J. Calvo, R. Kötz, O. Haas, A Probe Beam Deflection Study of Ion Exchange at Poly(vinylferrocene) Films in Aqueous and Nonaqueous Electrolytes, Langmuir 18 (2002) 2756–2764.
[10] C. Odin, M. Nechtschein, Memory effect in conducting polymers: Electrochemical and ESR studies on polyaniline, Synth. Met. 43 (1991) 2943–2946.
[11] C. Barbero, R. Kötz, M. Kalaji, L. Nyholm, L.M. Peter, Ion exchange and memory effects in polyaniline, Synth. Met. 55 (1993) 1545–1551.
[12] J.-P. Diard, N. Glandut, B. Le Gorrec, C. Montella, EIS study of the FeIII/FeII redox couple at a Nafion-coated Pt electrode, Journal of Electroanalytical Chemistry 566 (2004) 269–280.
[13] M.F. Dautartas, E.F. Bowden, J.F. Evans, Chemical and mechanical properties of redox polymer-modified electrodes, Journal of Electroanalytical Chemistry and Interfacial Electrochemistry 219 (1987) 71–89.
[14] C. Barbero, E.J. Calvo, R. Etchenique, G.M. Morales, M. Otero, An EQCM electroacoustic study of poly(vinylferrocene) modified electrodes in different aqueous electrolytes, Electrochim. Acta 45 (2000) 3895–3906.
[15] P.J. Peerce, A.J. Bard, Polymer films on electrodes, Journal of Electroanalytical Chemistry and Interfacial Electrochemistry 108 (1980) 121–125.
[16] M.N. Szentirmay, C.R. Martin, Ion-Exchange Selectivity of Nafion Films on Electrode Surfaces, Anal. Chem. 56 (1984) 1898–1902.
[17] G. Decher, J.-D. Hong, Buildup of ultrathin multilayer films by a self-assembly process, consecutive adsorption of anionic and cationic bipolar amphiphiles on charged surfaces, Macromolecular Symposia 46 (1991) 321–327.
[18] K.K. Kanazawa, A.F. Diaz, R.H. Geiss, W.D. Gill, J.F. Kwak, J.A. Logan, J.F. Rabolt, G. B. Street, Organic metals: polypyrrole, a stable synthetic 'metallic' polymer, J. Chem. Soc., Chem. Commun. (1979) 854–855.
[19] K.A. Striebel, G.G. Scherer, O. Haas, Effect of curing-humidity on recast-nation films, Journal of Electroanalytical Chemistry and Interfacial Electrochemistry 304 (1991) 289–296.
[20] P.J. Peerce, A.J. Bard, Polymer films on electrodes, Journal of Electroanalytical Chemistry and Interfacial Electrochemistry 112 (1980) 97–115.
[21] E.J. Calvo, V. Flexer, M. Tagliazucchi, P. Scodeller, Effects of the nature and charge of the topmost layer in layer by layer self assembled amperometric enzyme electrodes, Phys. Chem. Chem. Phys. 12 (2010) 10033–10039.
[22] P.J. Peerce, A.J. Bard, Polymer films on electrodes, J. Electroanal. Chem. Interfac. Electrochem. 114 (1980) 89–115.
[23] W.T. Yap, R.A. Durst, Effects of resistance and capacitance on the chronoamperomety of polymer-coated electrode as modeled by a finite elements digital simulation, J. Electroanal. Chem. 216 (1987) 11–19.
[24] K.L. Knoche, C. Hettige, P.D. Moberg, S. Amarasinghe, J. Leddy, Cyclic Voltammetric Diagnostics for Inert, Uniform Density Films, J.Electrochem. Soc. 160 (2013) H285–H293.
[25] M.D. Levi, R. Demadrille, A. Pron, M.A. Vorotyntsev, Y. Gofer, D. Aurbacha, Application of a Novel Refinement Method for Accurate Determination of Chemical Diffusion Coefficients in Electroactive Materials by Potential Step Technique, J. Electrochem. Soc. 152 (2005) E61–E67.
[26] N.A. Peppas, in: N.A. Peppas (Ed.), Hydrogels in medicine and pharmacy, vol. 2, CRC Press Inc., Boca Raton, Florida, 1986.
[27] N.A. Peppas, J.Z. Hilt, A. Khademhosseini, R. Langer, Hydrogels in Biology and Medicine: From Molecular Principles to Bionanotechnology, Adv. Mater 18 (2006) 1345–1360.
[28] H.H. Tuson, L.D. Renner, D.B. Weibel, Polyacrylamide hydrogels as substrates for studying bacteria, Chem. Commun. 48 (2012) 1595–1597.
[29] L.B. Gregor, Metal?Polyelectrolyte Complexes. I. The Polyacrylic Acid?Copper Complex, J. Phys. Chem. 59 (1955) 34–39.
[30] E.M. Ahmed, Hydrogel Preparation, characterization, and applications: A review, Journal of Advanced Research 6 (2015) 105–121.
[31] Z.M.O. Rzaev, S. Dinçer, E. Pişkin, Functional copolymers of N-isopropylacrylamide for bioengineering applications, Progress in Polymer Science 32 (2007) 534–595.
[32] X. Sui, X. Feng, M.A. Hempenius, G.J. Vancso, Redox active gels: synthesis, structures and applications, J. Mater. Chem. B 1 (2013) 1658–1672.
[33] H. Dahms, Electronic conduction in aqueous solution, J. Phys. Chem. 72 (1968) 362–364.
[34] I. Ruff, V.J. Friedrich, Transfer diffusion. I. Theoretical, J. Phys. Chem. 75 (1971) 3297–3302.
[35] F.I. Allen, L.R. Comolli, A. Kusoglu, M.A. Modestino, A.M. Minor, A.Z. Weber, Morphology of hydrated as-cast nafion revealed through cryo electron tomography, ACS Macro Lett 4 (2015) 1–5.
[36] W.L. Gellett, K.L. Knoche, N.P.W. Rathuwadu, J. Leddy, Electron Hopping of Tris (2,2 (bipyridyl) Transition Metal Complexes M(bpy)32/3 in Nafion, J. Electrochem. Soc. 163 (2016) H588–H597.
[37] R.E. Rivero, M.A. Molina, C.R. Rivarola, C.A. Barbero, Pressure and microwave sensors/actuators based on smart hydrogel/conductive polymer nanocomposite, Sensors and Actuators B: Chemical 190 (2014) 270–278.
[38] O. Okay, General Properties of Hydrogels, in: G. Gerlach, K.-F. Arndt (Eds.), Hydrogel Sensors and Actuators, Springer Series on Chemical Sensors and Biosensors 6, Springer-Verlag, Berlin Heidelberg, 2009.
[39] N. Annabi, J.W. Nichol, X. Zhong, C. Ji, S. Koshy, A. Khademhosseini, F. Dehghani, Controlling the Porosity and Microarchitecture of Hydrogels for Tissue Engineering, Tissue Eng Part B Rev 16 (2010) 371–383.
[40] R.E. Rivero, F. Alustiza, N. Rodríguez, P. Bosch, M.C. Miras, C.R. Rivarola, C.A. Barbero, Effect of functional groups on physicochemical and mechanical behavior of biocompatible macroporous hydrogels, React.Funct. Polym 97 (2015) 77–85.
[41] M.A. Molina, C.R. Rivarola, C.A. Barbero, Study on partition and release of molecules in superabsorbent thermosensitive nanocomposites, Polymer 53 (2012) 445–453.
[42] C.-A. Dai, C.-J. Chang, A.-C. Kao, W.-B. Tsai, W.-S. Chen, W.-M. Liu, W.-P. Shih, C.-C. Ma, Polymer actuator based on PVA/PAMPS ionic membrane: Optimization of ionic transport properties, Sensors and Actuators A 155 (2009) 152–162.
[43] M.V. Martinez, R. Coneo Rodriguez, A. Baena Moncada, C.R. Rivarola, M.M. Bruno, M.C. Miras, C.A. Barbero, Electrochemistry of Tris(1,10-phenanthroline)

iron(II) inside a polymeric hydrogel. Coupled chemical reactions and migration effects, J. Solid State Electrochemistry (2016), doi:http://dx.doi.org/10.1007/s10008-016-3312-6 in press.
[44] http://lem.ch.unito.it/chemistry/esp_manual.html (accessed 15.07.16).
[45] J.Q. Chambers, Chronocoulometric determination of effective diffusion coefficients for charge transfer trough thin electroactive polymer films, J. Electroanal. Chem. 130 (1981) 381–385.
[46] M.E.G. Lyons, H.G. Fay, T. McCabe, J. Corish, J.G. Vos, A.J. Kelly, Charge Percolation in Electroactive Polymer Films, J. Chem. Soc. Farad. Trans 86 (1990) 2905–2910.
[47] B.H. Meier, F. Graf, R.R. Ernst, Structure and dynamics of intramolecular hydrogen bonds in carboxylic acid dimers: A solid state NMR study, J. Chem. Phys. 76 (1982) 767–774.
[48] Z.X. Zhao, Z. Li, Q.B. Xia, E. Bajalis, H.X. Xi, Y.S. Lin, Swelling/deswelling kinetics of PNIPAAm hydrogels synthesized by microwave irradiation, Chem. Eng. J. 142 (2008) 263–270.
[49] K.S.V. Chen, Solution Redox Couples for Electrochemical Energy Storage I. Iron (lll)-Iron (11) Complexes with o-phenanthroline and related ligands, J. Electrochem. Soc. 128 (1981) 1467–1480.
[50] M.D. Luque de Castro, M. Valcarcel, F.N. Albahadyl, H.A. Mottola, Electrochemical behaviour of Iron-1,10-phenanthroline complexes at a carbon paste electrode, J. Electroanal Chem 219 (1987) 139–151.
[51] K. Ogura, K. Miyamoto, Electrode reaction of tris(1-10-phenanthroline)Iron(I) complex in aqueous and nonaqueous solvents, Electrochim. Acta 23 (1978) 509–512.
[52] H. Li, F. Lai, R. Luo, Analysis of Responsive Characteristics of Ionic-Strength-Sensitive Hydrogel with Consideration of Effect of Equilibrium Constant by a Chemo-Electro-Mechanical Model, Langmuir 25 (2009) 13142–13150.
[53] A.J. Bard, L.R. Faulkner, Electrochemical methods: fundamentals and applications, Wiley, New York, 1980.
[54] Y. Katayama, M. Yoshihara, T. Miura, Electrochemical Reaction of Tris(1,10-phenanthroline)iron Complexes in Some Amide-Type Ionic Liquids, J. Electrochem. Soc. 162 (2015) H501–H506.
[55] J.C. Myland, K.B. Oldham, Limiting currents in potentiostatic voltammetry without supporting electrolyte, Electrochem. Commun. 1 (1999) 467–471.
[56] L.K. Bieniasz, Analytical formulae for chronoamperometry of a charge neutralisation process under conditions of linear migration and diffusion, Electrochem. Commun. 4 (2002) 917–921.
[57] R. Lange, K. Doblhofer, The transient response of electrodes coated with membrane/type polymer films under conditions of diffusion and migration of the redox ions, J. Electroanal. Chem. 237 (1987) 13–26.
[58] M.T. Carter, M. Rodriguez M, A.J. Bard, Voltammetric studies of the interaction of metal chelates with DNA. 2. Tris-chelated complexes of cobalt(III) and iron (II) with 1,10-phenanthroline and 2,2'-bipyridine, J. Am. Chem. Soc. 111 (1989) 8901–8911.
[59] N. Oyama, S. Yamaguchi, Y. Nishiki, K. Tokuda, H. Matsuda, F.C. Anson, Apparent diffusion coefficients for electroactive anions in coatings of protonated poly(4-vinylpiridine) on graphite electrodes, J. Electroanal. Chem. 139 (1982) 371–382.
[60] L.A. Zook, J. Leddy, Density and Solubility of Nafion: Recast, Annealed, and Commercial Films, Anal. Chem. 68 (1996) 3793–3796.
[61] A. Einstein, Eine neue bestimmung der molecule dimensionen, Ann. Phys. 19 (1906) 289.
[62] M.M. Majda, L.R. Faulkner, J. Electroanal. Chem. 169 (1984) 77.
[63] C.L. Bentley, J. Li, A.M. Bond, J. Zhang, Mass-Transport and Heterogeneous Electron-Transfer Kinetics Associated with the Ferrocene/Ferrocenium Process in Ionic Liquids, J. Phys. Chem. C 120 (2016) 16516–16525.
[64] U. Pratap Azad, D. Kumar Yadav, V. Ganesan, F. Marken, Hydrophobicity effects in iron polypyridyl complex electrocatalysis within Nafion thin-film electrodes, Phys. Chem. Chem. Phys. 18 (2016) 23365–23373.
[65] J. Leddy, A.J. Bard, Polymer films on electrodes: Part XVIII. Determination of heterogeneous electron transfer kinetics at poly(vinylferrocene) and nafion/$Ru(bpy)_2{}^{+3}$ polymer-modified electrodes by convolution voltammetr, J. Electroanal. Chem 189 (1985) 203–219.
[66] N. Oyama, T. Ohsaka, M. Kaneko, K. Sato, H. Matsuda, Electrode kinetics of the $Fe(CN)_6{}^{4-/3-}$ and $Fe(CN)_5{}^{3-/2-}$ complexes confined to polymer film on graphite surfaces, J. Am. Chem. Soc. 105 (1983) 6003–6008.
[67] M.J. Weaver, Dynamical Solvent Effects on Activated Electron-Transfer Reactions: Principles Pitfalls, and Progress, Chem. Rev 92 (1992) 463–480.
[68] R.A. Marcus, Chemical and Electrochemical Electron-transfer theory, Annu. Rev. Phys. Chem. 15 (1964) 155–196.
[69] H.A. Zhang, R.W. Murray, Polymer Solvent Dynamic Effects on an Electron-Transfer Cross-Reaction Rate at a Redox Polymer/Polymer Solution Interface, J. Am. Chem. Soc. 115 (1993) 2335–2340.
[70] X. Zhang, J. Leddy, A.J. Bard, Dependence of Rate Constants of Heterogeneous Electron Transfer Reactions on Viscosity, J. Am Chem. Soc. 107 (1985) 3719–3721.
[71] M.E. Williams, J.C. Crooker, R. Pyati, L.J. Lyons, R.W. Murray, A 10^{11}-fold range of solvent dynamics control of heterogeneous electron transfers of cobalt(III/II)-tris(bipyridine), J. Am. Chem. Soc 119 (1997) 10249–10250.
[72] W. Miao, Z. Ding, A.J. Bard, Solution Viscosity Effects on the Heterogeneous Electron Transfer Kinetics of Ferrocenemethanol in Dimethyl Sulfoxide-Water Mixtures, J. Phys. Chem. B 106 (2002) 1392–1398.
[73] M. Hecht, W.R. Fawcett, Electrochemistry of [V(III)EDTA]- in Ethylene Glycol-Water Mixtures. 2. Kinetic Aspects: Solvation of the Transition State, J. Phys. Chem. 100 (1996) 14248–14255.
[74] R. Pyati, R.W. Murray, Solvent Dynamics Effects on Heterogeneous Electron Transfer Rate Constants of Cobalt Tris(bipyridine), J. Am. Chem. Soc 118 (1996) 1743–1749.
[75] M.A. Molina, C.R. Rivarola, C.A. Barbero, Evidence of Hydrophobic Interactions Controlling Mobile Ions Release from Smart Hydrogels, Mol. Cryst. Liq. Cryst. 512 (2010) 265–271.
[76] M.N. Szentirmay, C.R. Martin, Ion-Exchange Selectivity of Nafion Films on Electrode Surfaces, Anal. Chem. 56 (1984) 1898–1902.
[77] H. Braun, F. Decker, K. Doblhofer, H. Sotobayashi, The Redox-Reaction$[Fe(CN)_6]_3{}^{4-}$ on Electrodes Coated with Fixed Charge Polymer Films – Observation of Membrane Permeability Modulation by the Electrode Potential, Ber. Bunsenges. Phys. Chem 88 (1984) 345–350.
[78] Z. Qi, P.G. Pickup, Restructuring of cationic conducting polymers by $Fe(CN)_6{}^{4-}$, Journal of Electroanalytical Chemistry 441 (1998) 131–137.
[79] M.D. Ward, Ion exchange of ferro(ferri)cyanide in polyvinylferrocene films, J. Electrochem. Soc. 135 (1988) 2747–2750.
[80] E.L. Dewi, H. Nakano, K. Oyaizu, H. Nishide, E. Tsuchida, Ion-exchange and apparent diffusion coefficients within cationic polysulfonium coatings containing ferricyanide, J. Macromol. Sci. A 40 (2003) 37–47.
[81] S.M. Oh, L.R. Faulkner, Electron transport dynamics in partially quaternized poly(4-vinylpyridine) thin films containing ferri/ferrocyanide, J. Electroanal. Chem. 269 (1989) 77–97.
[82] R. Lange, K. Doblhofer, Membrane transport associated with double-layer charging of polymer modified electrodes, J. Electroanal. Chem. 216 (1987) 241–248.
[83] D. DeWulf, A.J. Bard, The diffusion of ferricyanide through perfluorinated ionomer (nafion) membranes, J. Macromol. Sci. A – Chemistry 26 (1989) 1205–1209.
[84] U. Pratap Azad, D. Kumar Yadav, V. Ganesan, F. Marken, Hydrophobicity effects in iron polypyridyl complex electrocatalysis within Nafion thin-film electrodes, Phys. Chem. Chem. Phys. 18 (2016) 23365–23373.
[85] U.P. Azad, V. Ganesan, Efficient sensing of nitrite by $Fe(bpy)_3{}^{2+}$ immobilized Nafion modified electrodes, Chem. Commun. 46 (2010) 6156–6158.
[86] A.A. Schilt, Analytical applications of 1,10-phenanthroline and related compounds, Pergamon Press, Oxford, 1969.
[87] C. Barbero, J.J. Silber, L. Sereno, Studies of surface-modified glassy carbon electrodes obtained by electrochemical treatmentts effect on $Ru(bpy)_3{}^{+2}$ adsorption and the electron transfer rates of the Fe^{2+}/Fe^{3+} couple, J Electroanal Chem 248 (1988) 321–340.
[88] U.P. Azad, S. Turllapati, P.K. Rastogi, V. Ganesan, Tris(1,10-phenanthroline)iron (II)-bentonite film as efficient electrochemical sensing platform for nitrite determination, Electrochimica Acta 127 (2014) 193–199.
[89] Y. Park, S. Kim, I.H. Jang, Y.S. Nam, H.i Hong, D. Choi, W.G. Lee, Role of the electric field in selective ion filtration in nanostructures, Analyst 11 (2007) 1109–1117.
[90] W. Bai, Q. Sheng, J. Zheng, Hydrophobic interface controlled electrochemical sensing of nitrite based on one step synthesis of polyhedral oligomeric silsesquioxane/reduced graphene oxide nanocomposite, Talanta 1 (2016) 302–309.
[91] U. Pratap Azad, V. Ganesan, Tris(4,4′-dimethyl-2,2(-bipyridine)iron(II)-Exchanged Nafion for Arsenite Determination in Water Samples, ChemElectroChem 1 (2014) 379–383.